

Methodologies for numerical modelling of prestressed concrete box-girder for long term deflection

M.C. Lalanthi^a, P. Kamatchi^{*}, K. Balaji Rao^b and S. Saibabu^c

CSIR-Structural Engineering Research Centre, Chennai - 600 113, India

(Received October 10, 2017, Revised December 1, 2017, Accepted December 6, 2017)

Abstract. In this paper, two methods M1 and M2 to determine long-term deflection through finite element analyses including the effect of creep and relaxation are proposed and demonstrated for a PSC box-girder. In both the methods, the effect of creep is accounted by different models from international standards viz., ACI-209R-92, CEB MC 90-99, B3 and GL2000. In M1, prestress losses due to creep and relaxation and age adjusted effective modulus are estimated through different models and have been used in finite element (FE) analyses for individual time steps. In M2, effects of creep and relaxation are implemented through the features of FE program and the time dependent analyses are carried out in single step. Variations in time-dependent strains, prestress losses, stresses and deflections of the PSC box-girder bridge through M1 and M2 are studied. For the PSC girder camber obtained from both M1 and M2 are lesser than simple bending theory based calculations, this shows that the camber is overestimated by simple bending theory which may lead to non-conservative design. It is also observed that stresses obtained from FEM for bottom fibre are lesser than the stresses obtained from bending theory at transfer for the PSC girder which may lead to non-conservative estimates.

Keywords: finite element model; prestressed concrete bridge girder; creep; relaxation

1. Introduction

Evaluation of long-term behaviour of prestressed concrete element is important from safety and serviceability concerns for which field monitoring is found to be appropriate. However, it is difficult to instrument the existing prestressed concrete beams/girders, hence finite element models are found to be suitable to evaluate time-dependent deflections. The importance of carrying out three dimensional finite element modelling of prestressed concrete elements has been identified in literature (Bazant *et al.* 2008, 2009). Analytical models do not account for shear stress variations within the cross section. Whereas FE modelling is useful in simulating field conditions and also to validate the field observations made, as a part of condition monitoring of existing prestressed concrete structures.

The segmental prestressed concrete box-girder of Koror-Babeldaob (KB) Bridge in Palau, which had the record span of 241 m, presents a striking paradigm of serviceability loss due to excessive multi-decade deflections (Bazant *et al.* 2008, 2009). As it is reported by Bazant *et al.* (2008) the segmental prestressed concrete box-girder of KB Bridge in Palau, erected segmentally in 1977, seems to have developed mid-span deflection of 1.61 m after 18 years, and

collapsed in 1996 even after remedial prestressing. From the comparison made for deflection of box-girder, it is reported that (Bazant *et al.* 2008), the traditional beam-type analysis has resulted in errors up to 20% compared to three-dimensional analysis, further it is stated that greater errors are likely for bridges with higher box width-to-span ratios.

Malm and Sundquist (2010) have analysed the cast-in-place construction of a balanced cantilever bridge with time-dependent material properties and showed that both deflection and stresses are higher than those originally assumed in the design calculations. Malm and Sundquist (2010) have stated that, when the box-girder bridges are traditionally analysed according to theory of bending the shear lag effect in the slabs due to the dead weight and the prestress are neglected which may lead to a considerable underestimation of the long-term deflections of box-girder bridges. It is suggested that use of 3D finite element (FE) model consisting of shell or solid elements can automatically capture the effect of shear lag and the effects of differential shrinkage and drying creep if suitable material descriptions are used. Therefore, it is important to carry out three dimensional analyses of prestressed concrete beam/bridge including the effect of creep and shrinkage for long-term deflection. Yang (2007) have proposed a method for the improvement of long-term prediction of time-dependent effects due to the creep and shrinkage of concrete by conducting short-term measurements at the early stage. The authors have also mentioned about ACI Committee 209 and the CEB-FIP MC 90 models for modelling of uncertainty of creep and shrinkage of concrete. Guo *et al.* (2011) have shown that the concrete creep and shrinkage dominates during the early stage of bridge structure deterioration. The time-dependent reliability assessment is

*Corresponding author, Principal Scientist
E-mail: kamat@serc.res.in

^aM. Tech Project Student

^bSr. Principal Scientist

^cChief Scientist

made for composite prestressed concrete box-girder bridge. Authors have also concluded that the recently developed GL2000 model, the CEB-FIP model, the B3 model and the ACI-209 model are more reliable than the earlier creep models. Goel *et al.* (2007) have briefly described some of the recent models which are based on the extensive research and experimental studies for prediction of creep and shrinkage. It is stated that the early mathematical models were developed with a view to facilitate structural analysis and the recent modelling methods focus on experimental data as closely as possible due to the ease of computation. Yeghneem *et al.* (2017) studied the seismic performance of RC shear walls strengthened by CFRP plates through numerical modeling of the aging effects viz., creep and shrinkage. Xihua *et al.* (2017) have studied the creep behavior of segmental box girder bridge. Wang *et al.* (2016) studied the effect of concrete age and creep on the behavior of concrete-filled steel tube columns. Ghasemzadeh *et al.* (2016) have demonstrated the procedure for predicting long-term compressive creep of concrete using inverse analysis method. Canovic and Goncalves (2005) have described the creep-related problems in ABAQUS with two different material models, either the material model creep or by using a visco-elastic description, visco. According to which the material model creep in ABAQUS is not suitable for the analysis of concrete if the stresses vary and especially not if it involves unloading. Because of this, creep has been modeled with the visco-elastic material definition visco and a quasi-static numerical integration. It is stated that, for concrete in reality, this is not the case, still, this way of modelling was considered to be appropriate for the concrete in the FE model and was therefore can be used.

From the brief review of literature, it is seen that it is necessary to carry out three dimensional finite element analyses of prestressed concrete members for prediction of long term deflection including the effect of creep and relaxation. Modelling and analysis PSC beam/bridge using finite element method (FEM) is a complex task. FEM is used to solve problems involving complex material properties and boundary conditions, wherein the structure is considered as an assemblage of finite elements interconnected at the joints by nodes. No study is reported in literature illustrating 3D FE analyses of PSC beam and girder including the effect of creep and relaxation for Indian conditions. In this paper, two methods viz., step by step analyses (designated as M1) and single step method (designated as M2) for three dimensional FE analyses of prestressed concrete beam and box-girder bridge to determine time-dependent strains, prestress losses, stresses and deflections are demonstrated. The results from 3D FE analyses are compared with deflections obtained by simple bending theory and the percentage differences brings out the importance of carrying out 3D FE analyses for PSC members.

2. Time-dependent analysis for prestressed concrete structure

The time-dependent analysis of PSC structures should include the long-term effects like creep, relaxation and

shrinkage of concrete which contribute in the excessive deflection and lead to loss of serviceability of structures. However, in the present study creep and relaxation effects are only implemented in finite element analyses and shrinkage effects are not considered both in M1 and M2.

2.1 Method M1

In method M1, the time-dependent step-by-step analysis of PSC girder is carried out by first estimation of creep coefficients using models available in international standards (Kamatchi *et al.* 2014) viz., ACI-209R-92 (ACI 2010), CEB MC90 (CEB 1993, CEB 1999), GL2000 (Gardner 2000, Gardner and Lockman 2001), B3 (Bazant and Baweja 1995, Bazant and Baweja 2000), for various time durations (age of concrete) considered. Using the estimated values of creep coefficients, the loss in the applied prestressing force is calculated. The time-dependent prestressing loss due to relaxation of steel is estimated. FE analyses is carried out for each age of concrete considered, with reduced prestress after accounting for losses at that age. In addition, age adjusted effective modulus is used to account for creep effects in each time duration (Bazant 1972). In this method, creep strains and losses are estimated using Eq. (1) for different creep models and relaxation losses over the time interval t_1 and t are estimated for stress relieved steel using Eq. (2).

$$\begin{aligned}\epsilon_{cr} &= f_i/E_c \times \phi(t, t_o) \\ f_{cr} &= \epsilon_{cr} \times E_s\end{aligned}\quad (1)$$

$$\% \text{ Loss of stress} = f_{cr}/f_{st} \times 100$$

$$RET = f_{st} \left(\frac{\log 24t - \log 24t_1}{10} \right) \left(\frac{f_{st}}{f_{py}} - 0.55 \right) \quad (2)$$

Where $\frac{f_{st}}{f_{py}} - 0.55 \geq 0.05$ and $f_{py} = 0.85f_{pu}$

2.2 Method M2

In method M2, the time dependent creep and relaxation effects are accounted by means of visco-elastic material model built-in ABAQUS (Hibbit *et al.* 2010). However, the input parameters for viscoelastic material model are obtained from creep models available in international standards viz., ACI-209R-92, CEBMC90, GI2000, B3. Time dependent elastic modulus of concrete from age adjusted effective modulus is also included in method M2. Analysis of structure is carried out in a single step.

2.2.1 Modelling of concrete

The time-dependent analysis of M2 for creep can be described in ABAQUS with two different material models, either the material model creep or by using a visco-elastic description, visco. According to Canovic and Goncalves (2005) the material model creep in ABAQUS is not suitable for the analysis of concrete if the stresses vary and especially not if it involves unloading. Because of this, creep in this study has been included in the model with the visco-elastic material definition visco and a quasi-static

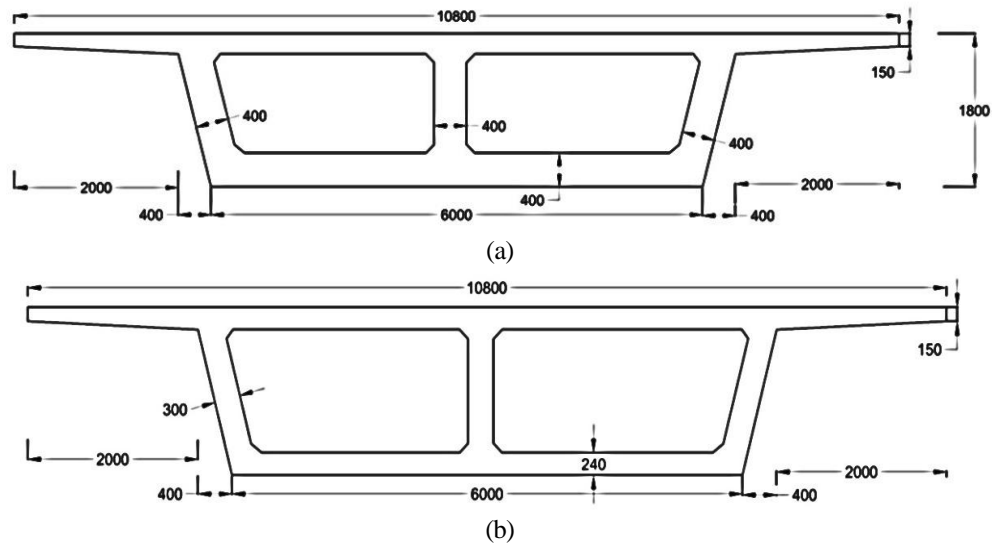


Fig. 1 Cross-section of box girder at (a) support (b) mid-span (All dimensions are in mm)

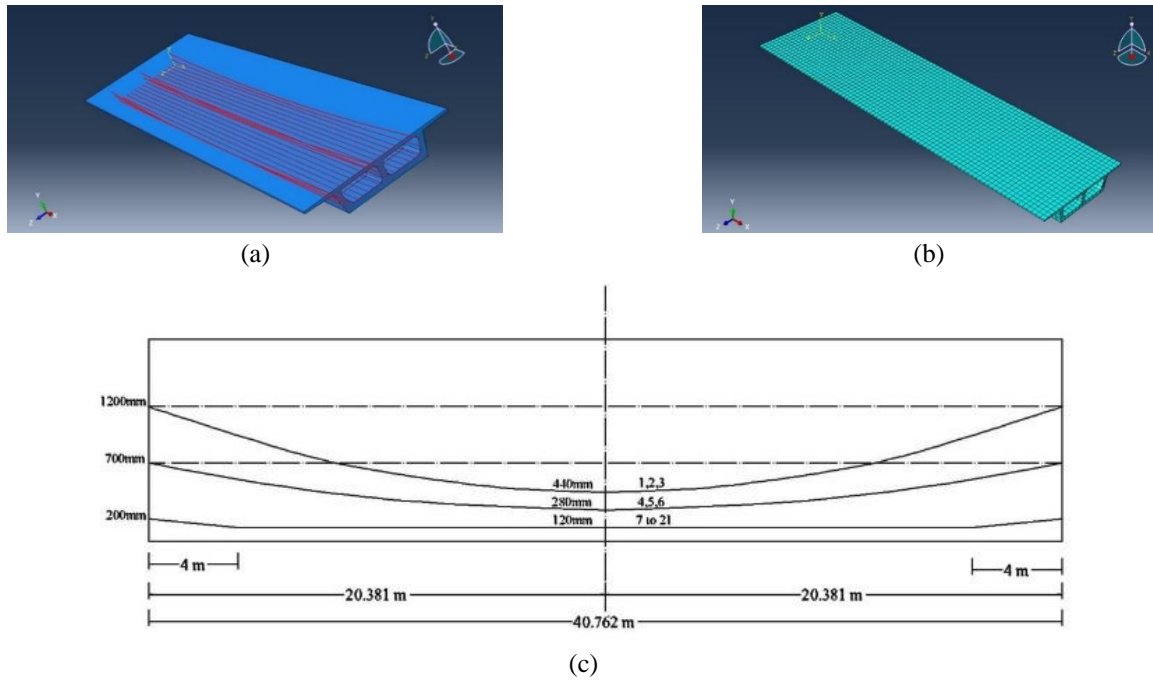


Fig. 2 FE model of box girder (a) Assembled box girder with tendons (b) The finite element mesh chosen for the present study (c) Sketch showing the Y-ordinates of cable (not to scale)

numerical integration. In the present study, the relaxation test data are used to specify the visco-elastic behaviour. The normalised shear and bulk moduli, $gR(t)$ and $kR(t)$, are defined as functions of the creep coefficient as given in Eqs. (3)-(4). Where the instantaneous bulk and shear modulus K_o and G_o are estimated using Eqs. (5) and (6).

$$gR(t) = \frac{G_R(t)}{G_o} = \frac{\frac{E_o}{2(1+\gamma_o)(1+\phi(t,t_o))}}{\frac{E_o}{2(1+\gamma_o)}} \quad (3)$$

$$gR(t) = \frac{1}{(1+\phi(t,t_o))}$$

$$kR(t) = \frac{K_R(t)}{K_o} = \frac{\frac{E_o}{3(1-2\gamma_o)(1+\phi(t,t_o))}}{\frac{E_o}{3(1-2\gamma_o)}} \quad (4)$$

$$kR(t) = \frac{1}{(1+\phi(t,t_o))}$$

$$K_o = \frac{E_o}{3(1-2\gamma_o)} \quad (5)$$

$$G_o = \frac{E_o}{2(1+\gamma_o)} \quad (6)$$

2.2.2 Relaxation of steel

The relaxation of the prestressing tendons can be defined with the same visco-elastic material model that is used to define creep in concrete. Relaxation losses depend only on initial stress in prestressing force and type of steel. Relaxation is implemented as relaxation test data, with the normalized shear and bulk moduli, $gR(t)$ and $kR(t)$, defined as functions of the relaxation loss as given in Eq. (7).

$$gR(t) = \frac{G_R(t)}{G_o} = 1 - \chi \quad (7)$$

$$kR(t) = \frac{K_R(t)}{K_o} = 1 - \chi$$

where, $\chi = \frac{RET}{\sigma_i}$, σ_i is the absolute value of the initial prestress.

3. Geometric details of box-girder bridge

The dimensions and sectional properties of the box-girder considered in the present study are given in Table 1. The sectional properties of box girder bridge are different at mid-span and at support. Along the length of the girder, thickness of bottom flange varies from 400 mm to 240 mm over a length of 1800 mm (i.e., between 1800 and 3600 mm from support). The cross section details of box girder at support and at mid span are shown in Fig. 1.

4. Finite element modeling of box girder

Geometric modelling of PSC box-girder is done in two stages. In first stage the box-girder is modelled with the concrete properties, and at the second stage, the modelling of pre-stressed tendon with the pre-stressing steel properties

is carried out. The box girder and the tendons are modelled as shown in Fig. 2(a) with the ordinates of the cable shown in Fig. 2(c). The tendons are modelled as 3-D deformable solid wire elements and the 3-D solid box-girder is assembled with 3-D solid wire as shown in Fig. 2(a). The box girder is meshed as 20 noded hexahedral element consisting of 4674 elements. It is a quadratic brick element, with 20 nodes and reduced integration point. The finite element mesh chosen for the present study, is shown in Fig. 2(b). Pre-stressed tendons are subdivided into 2-noded truss elements consisting of 8400 bar elements. Sufficiency of mesh fineness has been validated by comparing the results with a finer mesh with 20829 hexahedral elements. It was observed that finer mesh would yield only a negligible improvement of the computed elastic deflections. Hence the mesh with 4674 hexahedral elements adopted in the present study has been found to be adequate.

4.1 Material models

The girder has been prestressed from both the ends with 21 cables of 19T/13 stress relieved steel. The initial prestressing force of 2110 kN is applied to each tendon. Due to lack of experimental data the nonlinear stress-strain curve of the tendon given by Devalapura *et al.* (1992) is adopted in the present study as shown in Fig. 3(a). The details of pre-stressing tendon, pre-stressing force and properties of concrete used for PSC box-girder are given in Table 2. The concrete has to be modelled differently for time-dependent step-by-step and single-step analysis. Concrete is modelled using 'concrete smeared cracking model' for M1, and is modelled using 'visco-elasticity model' for M2. To obtain stress-strain behaviour of concrete under uniaxial compression, the concrete strain ϵ_0 corresponding to peak stress f_c is usually around range 0.002-0.0035 as suggested in Indian standards for reinforced concrete IS 456 2000 (BIS 2000). The representative value of $\epsilon_0=0.0035$ is adopted in the present study. The Poisson's ratio ν_c of concrete under uniaxial compressive stress ranges from

Table 1 Dimensions of the bridge girder

Description	Value (mm)
Total length of box girder	40762
Depth of box girder	1800
c/c span between supports of box girder	39962
Overall width of box girder	10800
Clear carriage way width	7500
Overhanging length of deck slab	2000
Bottom width of box girder	6000
Thickness of top flange (Deck Slab) for central 6800mm width	240
Thickness of top flange (Deck slab) at edge	150
Bottom flange thickness at mid span	240
Thickness of webs at mid span	300
Thickness of webs at support	400 (upto 1800 mm from support along the length of the girder)
Thickness of bottom flange at each support	400 (upto 1800 mm from support along the length of the girder)

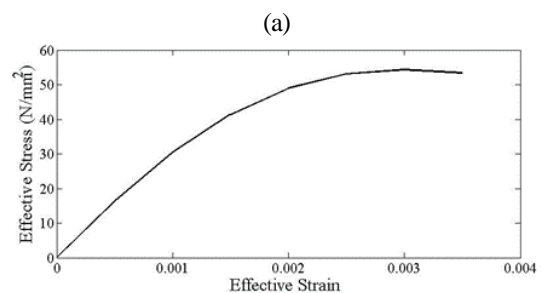
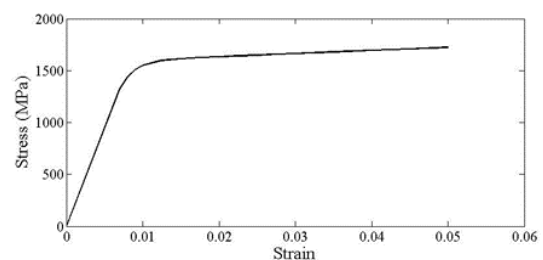


Fig. 3 Stress-strain curve (a) Pre-stressing tendon (b) Concrete (Equivalent uniaxial)

Table 2 Material properties adopted for pre-stressed tendon and concrete

Concrete material properties	
Yield stress (compression)=24750 kN/m ²	
Failure stress (compression)=42750 kN/m ²	
Plastic strain at failure (compression)=0.0015	
Tension Stiffening of Concrete for Concrete Smeared Cracking model	
σ/σ_c	$\varepsilon-\varepsilon_c$
1	0
0	0.002
Failure Ratio's	
Failure ratio	Value
Ratio 1	1.16
Ratio 2	0.0625
Ratio 3	1.28
Ratio 4	0.3333

Table 3 Properties of concrete for concrete smeared cracking model

Parameters adopted	
Elastic Modulus=1.95×10 ⁵ N/mm ²	
No of cables (19T/13) provided=21	
Area of each 19T/13 pre-stressing tendon=1765 mm ²	
Pre-stressing force provided for each cable (including instantaneous losses in pre-stressing force)=2110 kN	
Ultimate tensile strength of high tensile wire=2000 N/mm ²	
Elastic Modulus of concrete=38236760 kN/m ²	
Density of concrete=25 kN/m ³	
Poisson's Ratio of concrete=0.15	
Initial stress in concrete at level of C.G. of pre-stressing steel=8783 kN/m ²	

about 0.15-0.22 and a value of 0.15 is adopted in the present study.

Effective stress σ_c and effective strain ε_c are used to relate plastic deformation. It can be correlated by means of equivalent uniaxial stress strain curve. The equivalent uniaxial stress-strain curve generated using stress-strain relationships proposed by saenz *et al.* (1964) for concrete is shown in Fig. 3(b). When cracking of concrete takes place, a smeared model is used to represent the discontinuous macrocrack behaviour. Properties adopted in the present study for concrete smeared cracking model are given in Table 3. For the box-girder simply supported boundary condition is adopted. Dead load of 25 kN/m³ is applied as a body force on the box-girder with pre-stressing force. In case of visco-elastic material model the additional step 'visco' is to be defined. The time period of 2000 days is mentioned in this analysis. Also, initial incrementation size, and creep/visco-elastic error tolerance is estimated on trial and error basis.

5. Methods of analysis

5.1 Step-by-step analysis - Method M1

The time-dependent step-by-step analysis of PSC box-girder is carried out by estimation of creep coefficients

Table 4 Parameters and values adopted for creep calculations

Parameters	Values
Volume to surface ratio, v/s in mm	242.4
Slump, S in mm	90
Relative humidity, RH	70%
Fine aggregate to total aggregate percentage, ϕ	33%
Air content, ζ	6%
Cement content, c , kg/m ³	424.77
Characteristic compressive strength, f_{ck} , N/mm ²	45
Water content, w , kg/m ³	191.15
Fine aggregate content, kg/m ³	594.69
Coarse aggregate content, kg/m ³	1189.38
Water-cement ratio, w/c	0.45
Aggregate-cement ratio, a/c	4.2

Table 5 Percentage loss of pre-stress in method M1

Days	ACI-209R	B3	CEB MC 90-99	GL2000
36	1.31	1.49	2.00	3.08
124	3.69	4.79	4.88	6.02
214	4.54	6.03	6.02	7.08
321	5.14	6.96	6.85	7.90
550	5.91	8.19	7.90	9.04
710	6.25	8.79	8.38	9.61
871	6.52	9.27	8.75	10.08
1061	6.78	9.74	9.09	10.54
1337	7.07	10.30	9.46	11.10
1470	7.19	10.53	9.61	11.33
1628	7.31	10.79	9.77	11.58
1807	7.44	11.04	9.93	11.83

Table 6 Age Adjusted Effective Modulus (N/mm²) in method M1

Days	ACI-209R	B3	CEB MC 90-99	GL2000
36	33560.4	32893.9	31173.4	28029.7
124	29029.0	25573.4	25306.2	22249.3
214	27685.3	23348.4	23389.0	20752.3
321	26825.6	21836.2	22110.3	19663.6
550	25832.6	19977.1	20629.1	18216.6
710	25414.0	19147.6	20024.7	17707.2
871	25100.9	18506.4	19589.5	17133.0
1061	24872.7	18060.7	19305.0	16610.3
1337	24592.4	17406.5	18925.4	16035.1
1470	24448.7	17115.1	18722.4	15694.1
1628	24336.0	16882.2	18579.5	15440.8
1807	24224.5	16646.6	18441.5	15153.1
36	33560.4	32893.9	31173.4	28029.7

using different models suggested in international standards viz., ACI- 209R, B3, CEB-MC 90-99 and GL2000 for various ages of concrete for which analysis is to be carried out. The values and parameters adopted for calculation of creep for PSC box-girder is given in Table 4. Using the estimated values of creep coefficients the loss in the applied pre-stressing force is calculated. The time-dependent pre-stressing loss due to relaxation of steel is estimated. The total loss in pre-stressing force due to concrete creep and relaxation of steel is given in Table 5. The time-dependent age adjusted effective modulus for various ages is calculated

Table 7 Dimensionless normalized shear and bulk relaxation modulus for method M2

Days	ACI-209R		B3		CEB MC 90-99		GL2000	
	g_R	k_R	g_R	k_R	g_R	k_R	g_R	k_R
30	0.954	0.954	0.920	0.920	0.896	0.896	0.845	0.845
36	0.878	0.878	0.836	0.836	0.815	0.815	0.733	0.733
40	0.860	0.860	0.816	0.816	0.796	0.796	0.711	0.711
Typical values								
1500	0.639	0.639	0.446	0.446	0.489	0.489	0.409	0.409
1628	0.636	0.636	0.442	0.442	0.486	0.486	0.404	0.404
1750	0.634	0.634	0.437	0.437	0.483	0.483	0.399	0.399
1807	0.634	0.634	0.435	0.435	0.482	0.482	0.396	0.396
2000	0.631	0.631	0.430	0.430	0.479	0.479	0.391	0.391

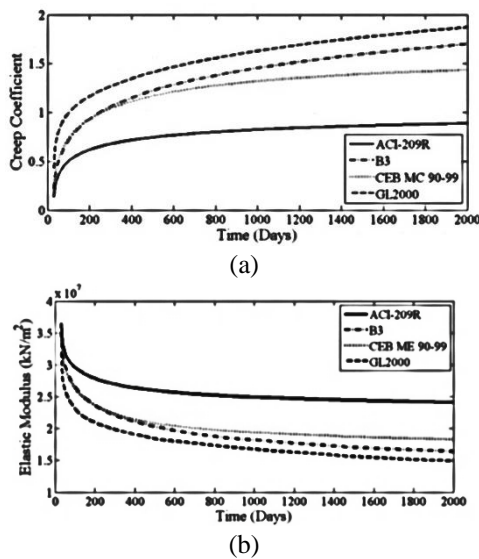


Fig. 4 Time dependent creep coefficient and age adjusted elastic modulus values for different models (a) Creep coefficient (b) Elastic modulus

using the estimated creep coefficients as given in Table 6. The time-dependent step-by-step analysis is carried out with the modified values of elastic modulus and with the reduced pre-stressing force after accounting for the instantaneous losses (i.e., due to elastic shortening, anchorage slip and friction) and losses due to creep and relaxation. The stresses and deflection are obtained for each time-step.

5.2 Single step analyses -Method M2

To carry out the time-dependent single-step analysis, the visco-elastic material model for concrete is used. The 'Time Points' are defined at the time of interest for which the output is obtained in a single-step analysis. The typical values of dimensionless normalized shear and bulk relaxation modulus values obtained for different models are given in Table 7. The time dependent elastic modulus is also calculated. To include the effect of change in elastic modulus in the finite element analysis, a field variable is introduced corresponding to time in ABAQUS. The variations in elastic modulus and creep coefficient with time for various models are shown in Fig. 4. The time-dependent single-step analysis is carried out by applying the initial

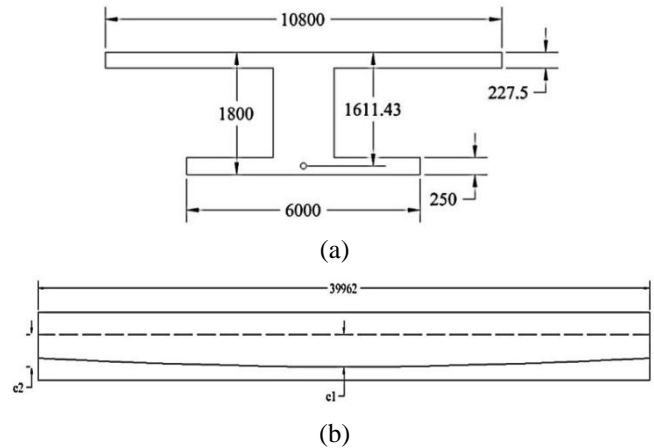


Fig. 5 Equivalent section for deflection calculation based on simple bending theory (a) Equivalent I-section for Box-girder (b) Locus of centroid of pre-stressing cable

pre-stressing force to the tendons. The analysis is carried out in single-step for all time steps (age of concrete) and the stresses in pre-stressed tendons are obtained to calculate the loss of pre-stress at required time, also the variation of stress across the cross-section with the deflection are obtained for each time-step.

6. Deflection calculation by simple bending theory

The deflection calculations are made for the box-girder considering it as a simple I-section for the box-section as shown in Fig. 5(a). For calculation of camber, simply supported beam with constant pre-stressing force and constant sectional properties are considered. The locus of centre of gravity of pre-stressing cable is shown in Fig. 5(b). Eccentricity at mid span w.r.t centre of gravity of concrete (e_1) is 859.819 mm and eccentricity at end w.r.t centre of gravity of concrete (e_2) is 634.104 mm. The dead load is applied as uniformly distributed load, and the pre-stressing force is assumed to be applied to the equivalent parabolic tendon. The mid span deflection and camber due to prestressing force are computed using Eqs. (8), (9). The deflections are calculated for all models using time-dependent E_t and P_t using simple bending theory.

$$\delta_d = \frac{5wl^4}{384E_c I} \quad (8)$$

$$\delta_c = \frac{P_t l^2}{8E_t I} \left[e_2 + \frac{5}{6}(e_1 - e_2) \right] \quad (9)$$

7. Observations

7.1 Time-dependent stresses through M1

The variation of stresses along the cross-section obtained through M1 for the flanges and webs for all the four creep models considered are plotted for 36 days and

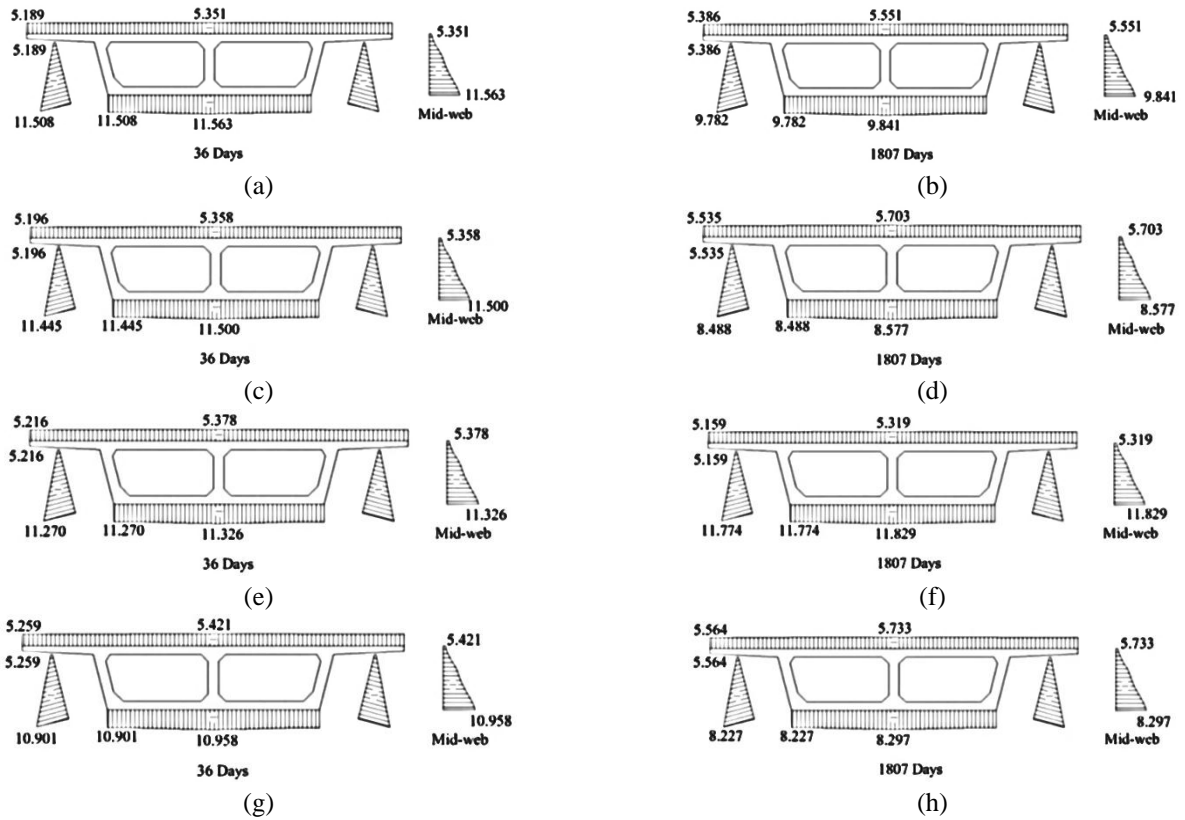


Fig. 6 Stress (N/mm²) distribution along the cross-section from M1 for (a) ACI-209R model – 36 days (b) ACI-209R model 1807Days (c) B3 model – 36 days (d) B3 model -1807Days (e)CEB MC 90-99 model -36 days (f) CEB MC 90-99 model – 1807 days (g) GL2000 model – 36 days (h) GL2000 model -1807 days

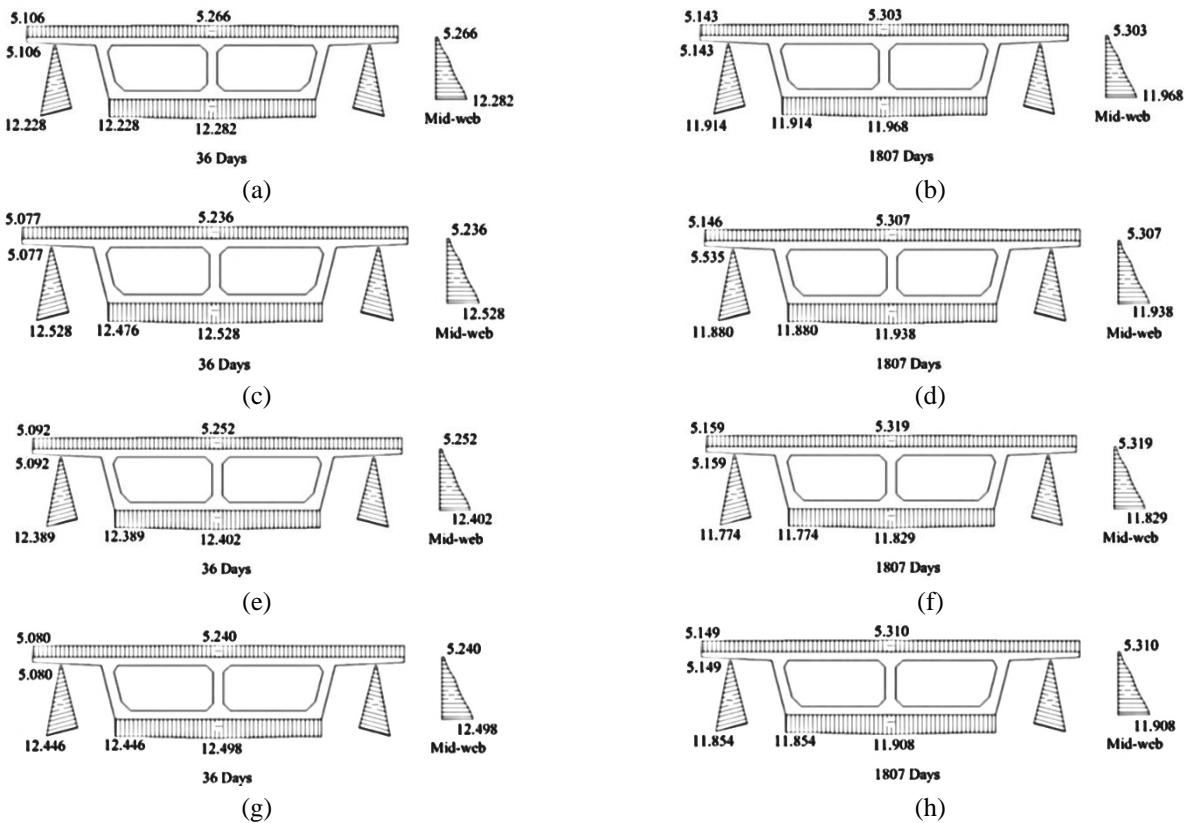


Fig. 7 Stress (N/mm²) distribution along the cross-section from M2 for (a) ACI-209R model – 36 days (b) ACI-209R model 1807Days (c) B3 model – 36 days (d) B3 model -1807Days (e) CEB MC 90-99 model -36 days (f) CEB MC 90-99 model – 1807 days (g) GL2000 model – 36 days (h) GL2000 model -1807 days

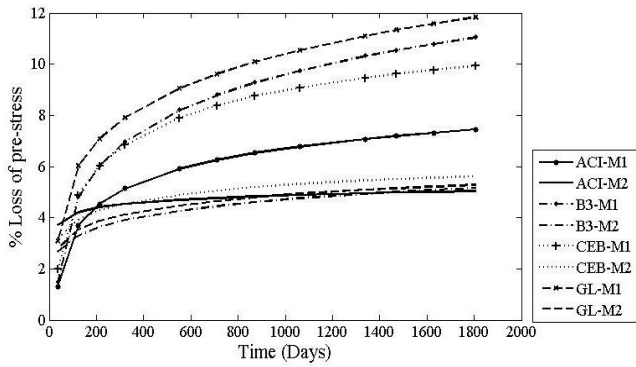


Fig. 8 Plot of percentage loss of pre-stress with time for M1 and M2

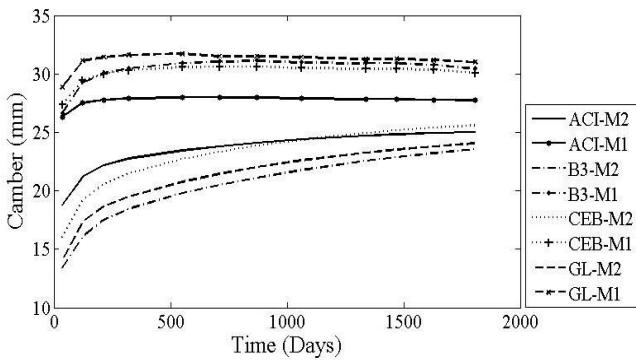
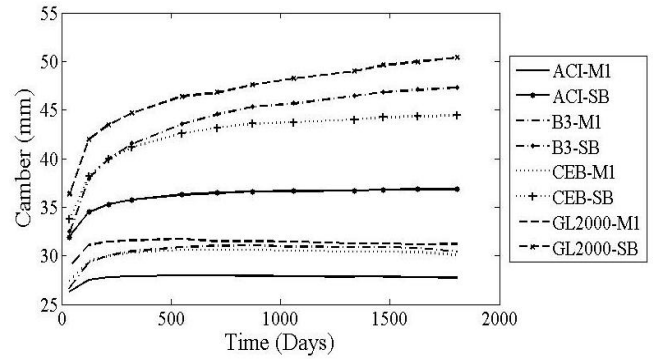


Fig. 9 Time-dependent camber obtained by different models using M1 and M2

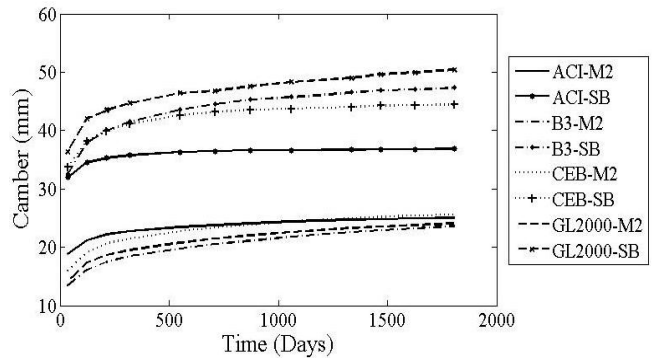
1807 days as shown in Figs. 6(a)-(h). It is seen from the figures that the stresses at the top flange increase with time and stresses in the bottom flange decreases with time. It is observed that there is a small variation of stress along the length of top and bottom flange. The time dependent stresses in the web are compared with the stresses at top and bottom fibre at transfer reported in design report as 4.895 N/mm² and 13.80 N/mm² respectively (Appa Rao *et al.* 1995). Stresses obtained from FE analysis from M1 and M2 are about 5.297 N/mm² and 12.01 N/mm² respectively in compression. It is seen that stresses increase over time in the top fibre and decrease over time in the bottom fibre.

7.2 Time-dependent stresses through M2

The variation of stresses along the cross-section for the flanges and webs for all the four creep models considered are plotted for 36 days and 1807 days as shown in Figs. 7 (a)-(h). It is seen from the figures that the stresses at the top flange increase with time and stresses in the bottom flange decreases with time. It is observed that there is a small variation of stress along the length of top and bottom flange. The plot of percentage loss of pre-stress obtained from M1 and M2 is shown in Fig. 8. The variation of percentage loss of pre-stress from M1 and M2 for all models increases with time. From Fig. 8 it can also be observed that GL2000 predicts higher percentage loss of pre-stress in both M1 and M2 compared to other models. Further from Fig. 8 it is seen that M1 predicts higher loss of



(a)



(b)

Fig. 10 Comparison of time-dependent camber obtained using simple bending theory and from FE analysis using different models (a) M1 (b) M2

pre-stress than M2 for all the models. Time-dependent camber obtained by different models using M1 and M2 are shown in Fig. 9. From Fig. 9 it is seen that, ACI-209R model predicts higher camber compared to other models for M2 and GL2000 model predicts higher camber compared to other models for M1. From Fig. 9 the camber obtained from M1 is found to be higher than M2 the maximum percentage variation of camber over the time is observed to be 28% for ACI-209R-92, 49% for B3, 41% for CEB MC 90-99 and 51% for GL2000 at 36 days.

The comparisons of time dependent deflections through M1 and M2 with deflections from simple bending theory (designated as SB) are shown in Figs. 10 (a) and (b) respectively. From Figs. 10 (a) and (b) it is seen that the variation of deflection between simple bending theory is higher for M1 and M2 i.e., SB predicts higher camber than M1, the maximum percentage of variation of camber with respect to SB over the time is observed to be 24% for ACI-209R, 35% for B3, 32% for CEB MC 90-99 and 38% for GL2000 at 1807 days. The similar comparison between, the variation of deflection between simple bending theory and M2, SB predicts higher camber than M2, the maximum percentage of variation of camber with respect to SB over the time is observed to be 41% for ACI-209R, 58% for B3, 52% for CEB MC 90-99 and 61% for GL2000 at 36 days. Camber obtained from both M1 and M2 are lesser than simple bending theory based calculations, this shows that the camber is overestimated by simple bending theory which may lead to non-conservative design.

8. Conclusions

Importance of carrying out 3D FE analyses for long term deflection has been emphasized in literature. In this paper, two methods M1 and M2 to determine long-term deflection through finite element analyses including the effect of creep and relaxation are proposed and demonstrated for a PSC box-girder. In both the methods, the effect of creep is accounted by different models from international standards viz., ACI-209R-92, CEB MC 90-99, B3 and GL2000. In M1, prestress losses due to creep and relaxation and age adjusted effective modulus are estimated through different models and used in FE analyses for individual time steps. In M2, effects of creep and relaxation are implemented through the features of FE program and the time dependent analyses are carried out in single step. Variations in time-dependent strains, prestress losses, stresses and deflections of the PSC beam and PSC box-girder bridge through M1 and M2 are studied. Further deflections from 3D finite element analyses are compared with simple bending theory based calculations.

For PSC box-girder it is observed that GL2000 predicts the higher percentage loss of pre-stress in both M1 and M2 compared to other models. It is seen that M1 predicts higher loss of pre-stress than M2. CEB MC 90-99 model predicts higher camber compared to other models for M2 and GL2000 model predicts higher camber compared to other models for M1. Camber obtained from both M1 and M2 are found to be lesser than simple bending theory based calculations, this shows that the camber is overestimated by simple bending theory which may lead to non-conservative design. This observation brings out the necessity of carrying out 3D finite element analyses for estimation of long-term deflection.

In addition, the time dependent stresses across the cross section of beam and web of box-girder are obtained from 3D FE analyses and the comparison has been made with simple bending theory based calculations. It is seen that stresses increase over time in the top fibre and decreases over time in the bottom fibre. Further it is observed that, the stresses estimated from simple bending theory are more than the value obtained by FE Analysis at transfer at top and bottom fibre. It is also observed that stresses obtained from FEM for bottom fibre are lesser than the stresses obtained from bending theory at transfer which may lead to non conservative estimates. This study brings out importance of carrying out 3D finite element time dependent analyses for PSC members for long term deflection and stresses and demonstrates the procedures to carry out the same.

Acknowledgements

This paper is published with the kind permission of the Director, CSIR-Structural Engineering Research Centre, Chennai, India.

References

American Concrete Institute, (2010), ACI Manual of

- Concrete Practice, Part 1, USA.
- Appa rao, T.V.S.R., Narayanan, R., Prasadarao, A.S., Ravisankar, K., Ramanjaneyulu, K., Sreenath, H.G., Vimalanandam, V., Saibabu, S., Sukhesh, K.K. and Bhaskaran, R. (1999), "Design report for the replacement of superstructure of the flyover bridge across dumper lines of Visakhapatnam port trust", Visakhapatnam, Technical Report CSIR-SERC, Chennai.
- Bazant, Z.P. (1972), "Prediction of concrete creep using age-adjusted effective modulus method", *J. Am. Concrete Inst.*, **69**(4), 212-217.
- Bazant, Z.P. and Baweja, S. (1995), "Creep and shrinkage prediction model for analysis and design of concrete structures-model B3", *Mater. Struct.*, **28**, 357-365.
- Bazant, Z.P. and Baweja, S. (2000), "Creep and shrinkage prediction model for analysis and design of concrete structures: model B3", *The Adam Neville Symposium: Creep and Shrinkage-Structural Design Effects*, SP-194.
- Bazant, Z.P., Li, G.H., Yu, Q., Klein, G. and Kristek, V. (2008), "Explanation of excessive long-term deflections of collapsed record-span box girder bridge in Palau", *Preliminary report, 8th International Conference on Creep and Shrinkage of Concrete (CONCREEP-8)*, Ise-Shima, Japan.
- Bazant, Z.P., Li, G.H., Yu, Q., Klein, G. and Kristek, V. (2009), "Excessive long-time deflections of collapsed record-span box girder", *Structural Engineering Report No. 09-12/ITI*.
- Bureau of Indian Standards (2000), Indian Standard Plain and Reinforced Concrete Code of Practice IS 456: 2000, New Delhi, India.
- Canovic, S. and Goncalves, J. (2005), "Modelling of the response of the New Svinesund Bridge FE analysis of the arch launching", Master's Thesis Report, Department of Civil and Environmental Engineering, Chalmers University of Technology Göteborg, Sweden.
- CEB (1993), CEB-FIP Model Code 1990, CEB Bulletin d'Information No. 2131214, Comite Euro-International duBeton, Lausanne, Switzerland.
- CEB (1999), Structural Concrete-Textbook on Behaviour, Design and Performance, Updated Knowledge of the CEBI FIP Model Code 1990, fib Bulletin 2, V. 2, Federation Internationale du Beton, Lausanne, Switzerland.
- Devalapura, R.K. and Tadros, M.K. (1992), "Stress-strain modeling of 270 ksi low-relaxation prestressing strands", *PCI J.*, **37**(2), 100-106.
- Gardner, N.J. (2000), "Design provisions for shrinkage and creep of concrete", *The Adam Neville Symposium: Creep and Shrinkage-Structural Design Effects*, SP-194, Ed. A. AI-Manaseer, American Concrete Institute, Farmington Hills, MI.
- Gardner, N.J. and Lockman, M.J. (2001), "Design provisions for drying shrinkage and creep of normal strength concrete", *ACI Mater. J.*, **98**(2), 159-167.
- Ghasemzadeh, F., Manafpour, A., Sajedi, S., Shekarchi, M. and Hatami, M. (2016), "Predicting long-term compressive creep of concrete using inverse analysis method", *Constr. Build. Mater.*, **124**, 496-507.
- Goel, R., Kumar, R. and Paul, D.K. (2007), "Comparative study of various creep and shrinkage prediction models

- for concrete”, *J. Mater. Civil Eng.*, ASCE, **19**, 249-260.
- Guo, T., Sause, R., Frangopol, D.M. and Li, A. (2011), “Time-dependent reliability of PSC box-girder bridge considering creep, shrinkage, and corrosion”, *J. Bridge Eng.*, ASCE, **16**(1), 29-43.
- Hibbit, Karlson and Sorensen Inc. (2010), ABAQUS/CAE Version 6.10, User’s Manual, Theory Manual and Keywords Manual, U.S.A.
- Kamatchi, P., Rao, K.B., Dhayalini, B., Saibabu, S., Parivallal, S., Ravisankar, K. and Iyer, N.R. (2014), “Long-term prestress loss and camber of box girder bridge”, *ACI Struct. J.*, **111**(6), 1297-1306.
- Malm, R. and Sundquist, H. (2010), “Time-dependent analyses of segmentally constructed balanced cantilever bridges”, *Eng. Struct.*, **32**(4), 1038-1045.
- Saenz, L.P. (1964), Discussion of “equation for the stress-strain curve of concrete, by Desayi P. and Krishnan S”, *ACI J.*, **61**, 1229-1235.
- Wang, H.Y., Zha, X.X. and Feng, W. (2016), “Effect of concrete age and creep on the behavior of concrete-filled steel tube columns”, *Adv. Mater. Sci. Eng.*, **2016**, Article ID 7261816, 10.
- Xihua, D., Liangfang, L. and Rong, X. (2017), “Creep behavior of precast segmental box girder bridge”, *IOP Conference Series: Earth and Environmental Science*, **81**, 012138. 10.1088/1755-1315/81/1/012138.
- Yang, I.H. (2007), “Prediction of time-dependent effects in concrete structures using early measurement data”, *Eng. Struct.*, **29**, 2701-2710.
- Yeghnem, R., Guerroudj, H.Z., Amar, L.H.H., Meftah, S.A., Benyoucef, S., Tounsi, A. and Bedia, E.A.A. (2017), “Numerical modeling of the aging effects of RC shear walls strengthened by CFRP plates: A comparison of results from different “code type” models”, *Comput. Concrete*, **19**(5), 579-588.

E_o	= Instantaneous elastic modulus
ν_o	= Instantaneous Poisson’s ratio
$\phi(t, t_o)$	= Creep coefficient
l	= span of the girder in m
w	= self weight of the girder per metre run
δ_d	= Down ward deflection
δ_c	= Upward deflection due to prestressing force
ϵ_o	= Concrete strain corresponding to peak stress
ϵ_{cr}	= creep strain in concrete
σ_o	= Concrete strain corresponding to peak stress
σ_c	= Effective strain in concrete
E_t	= Time-dependent elastic modulus
P_t	= Time dependent prestressing force

CC

Symbols

E_c	= Modulus of elasticity of concrete in MPa
E_s	= Modulus of elasticity of steel in MPa
f_i	= Initial stress in concrete at the level of C.G. of prestressing steel in MPa
f_{st}	= Initial stress in steel in MPa
f_{pu}	= Ultimate tensile strength of prestressing steel in MPa
f_{py}	= Yield Strength of prestressing steel in MPa
t	= Age of concrete considered in days
t_o	= Age of concrete when loading starts in days
RET	= loss due to relaxation
ϵ_c	= Effective strain in concrete
$g_R(t)$	= Normalised shear modulus
$k_R(t)$	= Normalised bulk modulus
$G_R(t)$	= Shear modulus
$K_R(t)$	= Bulk modulus
G_o	= Instantaneous shear modulus
K_o	= Instantaneous bulk modulus